SIZE EFFECT FOR FLEXURAL COMPRESSION OF CONCRETE SPECIMENS

J. K. Kim
Department of Civil Engineering, Korea Advanced Institute of Science and Technology, Korea
S. T. Yi
Department of Civil & Structural Engineering, Korea Power Engineering Company, Inc., Korea
E. I. Yang
Coastal and Harbor Engineering Research Center, Korea Ocean Research and Development Institute, Korea
S. H. Eo
Department of Civil Engineering, Changwon National Univ., Korea

Abstract
In this study, the size effect of concrete members subjected to the axial load and bending moment is investigated using a series of C-shaped specimens of which test procedure is similar to those of Hognestad, Hanson, and McHenry. Main test variable is a size ratio of the specimens(1:1/2:1/4) at the concrete compressive strength of 50 MPa.

Test results show that the flexural compression strength at failure decreases as the size of specimen increases, that is, the size effect law is present. Model equation is derived using regression analyses with experimental data; it is felt that they perform better than Bazant's model. Additionally, it is observed that there is a slight increase in elastic modulus and relative decrease in strains corresponding to the maximum stress of C-shaped specimens compared to those of cylindrical specimens.

Further experimental study will involve changing of concrete compressive strength to determine its effect at the other strength.
Key words: Size effect, C-shaped specimen, axial load, bending moment

1 Introduction

The inelastic stress distribution in the concrete compression zone of flexural

members is more difficult to measure and express in mathematical terms. In 1955, Hognestad et al. presented concrete stress distribution in ultimate strength design by a rising curve from zero to maximum stress and a descending curve beyond the maximum stress. A test method using an eccentrically loaded C-shaped specimen was developed. These were adopted in the ACI code and the conditions are illustrated in Fig. 1.

After that this was experimentally supported by Kaar et al. and Swartz et al. using same test procedure and specimens and an ultimate strength design theory of application was developed by Mattock et al. based on an equivalent rectangular stress distribution. But, till now few papers were published due to difficulties encountered in performing experiments.
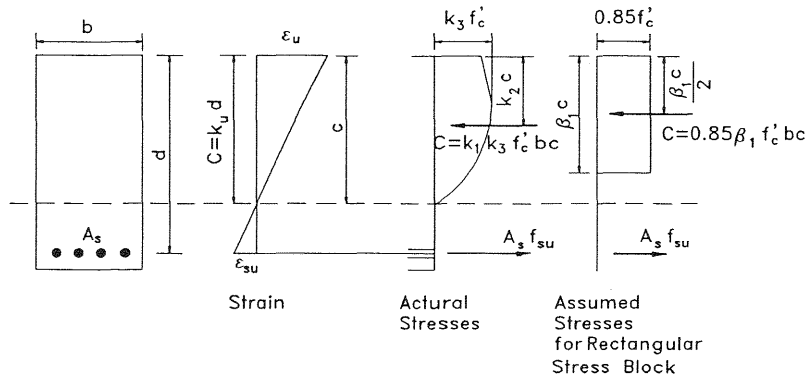

Fig. 1.   Conditions at ultimate load

In 1984, Bazant derived the size effect law from the dimensional analysis for geometrically similar members considering the energy balance at crack propagation in concrete as follows : ·

$$\sigma_n = \frac{P}{bd} = \frac{Bf_t'}{\sqrt{1 + \frac{d}{\lambda_o d_a}}} \tag{1}$$

Where, σ_n = nominal stress at failure, P = load or loading parameter, b = thickness, d = characteristic dimension, f_t' = direct tensile strength of concrete, d_a = maximum aggregate size, B and λ_o = empirical constants.

Many researches have been carried out to verify the fracture mechanics type size effect for various types of failure of concrete structures, for example, diagonal shear failure of beams, punching shear failure of slabs, pull out failure of bars, and failure of other structures.

Generally speaking, the size effect law was established by pure tension or pure compression etc. not flexural compression load condition. The reduction phenomena

of concrete compressive strengths and stress-strain curves with the size of C-shaped specimens is an intriguing phenomena, however, to date an analytical or experimental technique has not been found.

In this study, concrete members subjected to axial loads and bending moments were investigated to check the application of the size effect law on the compressive surface of flexural members. The series of specimens and test procedure employed are similar to those of Hognestad et al. The main test variable was a size ratio(1:1/2:1/4) of the specimens at the concrete compressive strength of 50 MPa. All were rectangular specimens with width b of 12.5 cm.

2 Test specimens and experimental procedure

2.1 Mix design

The mix proportions selected for the C-shaped specimens are given in Table 1. Specimens were cast horizontally on a level surface. Maximum aggregate size(d_a) was 13 mm and super-plasticizer and vibrator were used to consolidate the concrete.

Table 1. Concrete mix and properties

W/C (%)	S/a (%)	W	C	S	G	Sp[*] (%)
		(kg/m^3)				
37.0	40.0	177.6	480.0	676.0	1014.0	0.5

* Super-plasticizer weight is calculated based on cement weight

All cylinders and beam specimens were removed from the mold after 24 hrs and dry-cured under a wet burlap/towel before testing.

Table 2. Beam specimens

Notation	Testing age (days)	f_c' (MPa)	$P_{l,ulti}$ (KN)	Remarks
500-I-1	85		1088.91	
500-I-2	87		1114.81	
500-I-3	89		1058.79	
500-II-1	106		585.26	
500-II-2	113	56.31	598.31	
500-II-3	116		560.64	
500-III-1	46		-	Failed in bearing
500-III-2	56		317.35	
500-III-3	56		338.74	

The concrete compressive strength given in Table 2 is an average from three 10×20 cm cylinders per series. Cylinders were tested at the similar age with the specimens. The test ages are shown in Table 2.

Eight of specimens were tested successfully, that is failure occurred in the central test region and was in a compressive mode in which spalling preceded collapse. It ought to be noted that specimen number 500-III-1 was failed in bearing at its low end during test processing time and its data did not have any meaning.

Larger specimens tend to fail in a more brittle manner, while smaller specimens tend to fail in a less brittle manner. This is related to the release of energy stored in the testing machine, which in turn is related to the stiffness of the machine.

2.2 Details of test beams

The C-shaped specimen is shown in Fig. 2. The central test section of each specimen was not reinforced. Flexural and shear reinforcement was used in the two ends of the specimen.
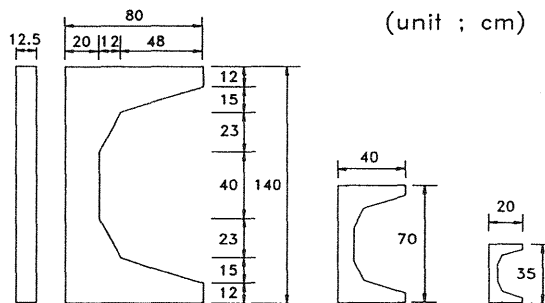

Fig. 2. Test specimens

During testing, strains were measured at mid-height of the test section by twelve 15.24 cm(6 in) strain gages. Two LVDTs were used to monitor the deflection of the center of test range relative to the ends. This information was used to adjust the load lever arm distances a_1 and a_2 for calculation of bending moment.

2.3 Testing procedure

The test setup is shown schematically in Fig. 3.

The major load, P_1, was supplied by a displacement controlled testing machine of 2500 KN capacity that is hydraulically operated. The minor load, P_2, was applied using a hand-operated hydraulic jack of 200 KN capacity. For the case of size III, P_2 was applied by using a rotating assembly.

Testing procedure was as follows : firstly, an increment of load P_1 was applied, and maintained while applying load P_2 and monitoring the value of strain gages on the tension face. On reaching zero strain value(on the average) the load P_2 was maintained while P_1 was increased further. This procedure was repeated until failure of members.
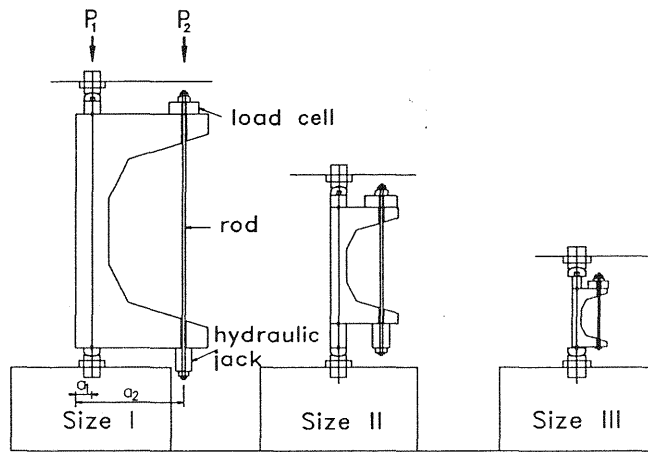
Fig. 3.   Test setup

2.4   Data reduction

Data reduction followed the procedure used by Hognestad et al. Using the assumption of linear strain distribution, the following equations are obtained from equilibrium of internal and external forces.

$$f_c = \varepsilon_c \frac{df_o}{d\varepsilon_c} + f_o \tag{2-1}$$

$$f_c = \varepsilon_c \frac{dm_o}{d\varepsilon_c} + 2m_o \tag{2-2}$$

where,

f_c = compressive stress in concrete
ε_c = strain in concrete
f_o = average compressive stress in concrete
     = $(P_1 + P_2)/bc$
m_o = applied moment/bc^2
     = $(P_1 a_1 + P_2 a_2)/bc^2$
b = width of rectangular member
c = distance from neutral axis to compressive edge of member

3   Test results

Values of outer fiber stresses, f_c obtained from averaging the results of Eqs. 2-1 and 2-2 are plotted against outer fiber strain values, ε_c in Fig. 4. The values obtained from

Eq. 2-1 and Eq. 2-2 were, in general, in agreement. It is assumed that the f_c-ε_c relationship thus estabilished is valid for all fibers in the beam. Thus a compressive stress can be determined from this and the measured strain.

Also plotted in this figure are the uniaxial compressive stress-strain curves for corresponding cylinders. In Fig. 4, the thin and thick solid lines are results from C-shaped beams and cylinders respectively. It is seen that although there are some obvious differences in size III, the overall agreement is quite good up to $f_c{}'$. It is possible to predict the behavior of beam specimens based on response of cylinder's stress-strain data with reasonable accuracy. It was noted, however, that elastic modulus of C-shaped specimens was slightly bigger than cylinders and strains corresponding to the maximum stress of C-shaped specimens decreased a little in comparison with those of cylinders.
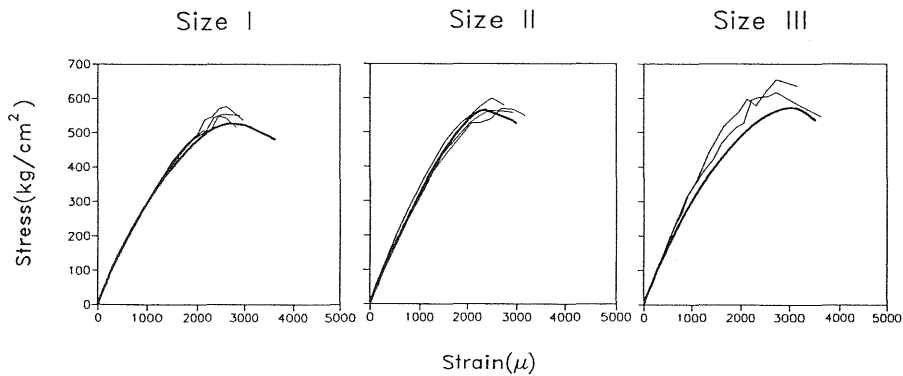

Fig. 4.   Comparisons of compressive stress-strain response in beam specimens and cylinders (1 kg/cm² = 0.0981 MPa)

Kim and Eo proposed a modified size effect law by adding the size independent strength $\sigma_o(=\alpha f_t{}')$ to the right side of Eq. 1 as follows.

$$\sigma_n = \frac{Bf_t{}'}{\sqrt{1 + \dfrac{D}{\lambda_o d_a}}} + \alpha f_t{}' \tag{3}$$

In order to obtain a model equation which can predict the flexural compression strength of C-shaped specimens at failure, regression analyses are carried out with 8 test data. Eq. 4 is obtained from the analyses, the results are given in Fig. 5.

$$\sigma_n = \frac{9.9 f_c{}'}{\sqrt{1 + 256 \dfrac{d}{d_a}}} + 0.6 f_c{}' \tag{4}$$

1998

From the equation neglected the second term of Eq. 4 which is the same as that proposed by Bazant, and by regression analyses with the same data, Eq. 5 is obtained.

$$\sigma_n = \frac{0.99 f_c{}'}{\sqrt{1 + \dfrac{d}{22.64 d_a}}} \tag{5}$$

Fig. 5 shows the value R_s as a function of ratio, R_c, of the distance from neutral axis to compressive edge of member. Here R_s means the ratio of stresses defined as $P_{l,ult}/bc$. In this Fig., dashed, thin and thick solid lines represent results from LEFM, Bazant's formula and Eq. 4 as illustrated.

It can be seen that, as a result of the specimen size, an increase of compressive strength follows in accordance with size effect law newly suggested by Eq. 4, which is dependent on the size of the member.
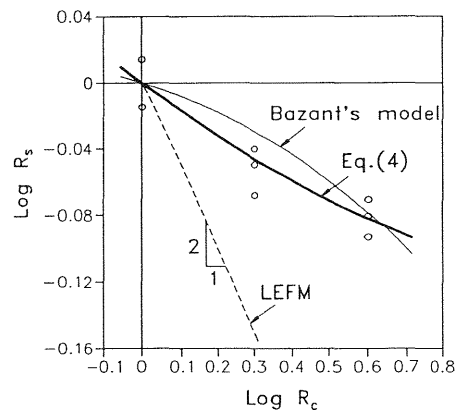

Fig. 5.　Comparison of Eq. (4) with others

4　Conclusions

A series of tests on twelve plain high strength concrete beams and associated cylinders at the concrete compressive strength of 50 MPa were carried out to check the application of size effect law on the compressive surface of flexural members. From the test results the following conclusions may be made.

1. A size effect is present, i.e. the flexural compression strength at failure decreases as the specimen size increases. New model equation is derived, it predict the reduction phenomena better than Bazant's model.
2. It is observed that there is a slight increase in elastic modulus and relative decrease in strains corresponding to the maximum stress of C-shaped specimens compared to those of cylindrical specimens.

5 Further experiment

Since this experimental study is still underway, these experimental results are not completed. Further experiment will involve the decrease and increase of concrete compressive strength to 25 and 80 MPa.

6 References

Bazant, Z.P., (1984) Size Effect in Blunt Fracture ; Concrete, Rock, Metal, **Journal of Engineering Mechanics, ASCE**, 110, 518-535.

Bazant, Z. P., and Cao. Z., (1986) Size Effect in Brittle Failure of Unreinforced Pipes, **ACI Journal**, 83, 369-373.

Bazant, Z. P., and Cao, Z., (1987) Size effect in Punching Shear Failure of Slabs, **ACI Structural Journal**, 84, 44-53.

Bazant, Z. P., and Kim, J. K., (1984) Size Effect in Shear Failure of Longitudinally Reinforced Concrete Beams, **ACI Journal**, 81, 456-468.

Bazant, Z. P., and Kwon, Y. W., (1994) Failure of Slender and Stocky Reinforced Concrete Columns: Tests of Size Effect, **Materials and Structures, Research and Testing** (RILEM, Paris), 27, 79-90.

Bazant, Z. P., and Sener, S., (1988) Size Effect in Pullout Tests, **ACI Materials Journal**, 85, 347-351.

Benjamin and Cornell, (1970) **Probability, Statistics, and Decision for Civil Engineers**, McGraw-Hill, New York, Section 4.3.

Hognestad, E., Hanson, N. W., and McHenry, D., (1955) Concrete Stress Distribution in Ultimate Strength Design, **Journal of ACI**, 52, 455-479, also **PCA Development** Bulletin D6.

IMSL, Library, Edition 8, IMSL, Inc.

Kaar, P. H., Hanson, N. W. and Capell H. T., (1977) Stress-Strain Characteristics of High-Strength Concrete, **PCA Research and Development** Bulletin RD051.01D, 1-10.

Kim, J.K., and Eo, S.H., (1990) Size Effect in Concrete Specimens with Dissimilar Initial Cracks, **Magazine of Concrete Research**, 42, 233-238.

Kim, J.K., Eo, S.H. and Park, H.K., (1989) Size Effect in Concrete Structures without Initial Crack, Fracture Mechanics ; **Application to Concrete, SP-118**, ACI, Detroit, 179-196.

Marti, P., (1989) Size Effect in Double-Punch Tests on Concrete Cylinders, **ACI Materials Journal**, 86, 597-601.

Mattock, A. H., Kriz, L. B. and Hognestad, E., (1961) Rectangular Concrete Stress Distribution in Ultimate Strength Design, **Journal of ACI**, 57, 875-928, also **PCA Development** Bulletin D49.

Swartz, S.E., Nikaeen, A., Narayan Babu, H.D., Periyakaruppan, N., Refai, T.M.E., (1985) Structural Bending Properties of Higher Strength Concrete, **High-Strength Concrete, SP-87, ACI**, 147-178.